Controllable 3D Plasmonic Nanostructures for High Quantum Efficiency UV Photodetectors Based on 2D and 0D Materials

Ming-Yu Li, [a,b] Muni Yu, [a] Shenglin Jiang, [a,b] Sisi Liu, [a] Hezhuang Liu, [c] Hao Xu, [c,d] Dong Su, [a] Guangzu Zhang, *[a,b] Yuntian Chen, [a] and Jiang Wu * [c,d]

[a]School of Optical and Electronic Information and Wuhan National Laboratory of Optoelectronics, Huazhong University of Science and Technology, Wuhan, Hubei 430074, China.

[b]Shenzhen Huazhong University of Science and Technology Research Institute, Shenzhen, Guangdong, 518057, China.

[c]Institute of Fundamental and Frontier Sciences, University of Electronic Science and Technology of China, Chengdu, Sichuan 610054, China.

[d]Department of Electronic and Electrical Engineering, University College London, London, WC1E 6BT, UK.

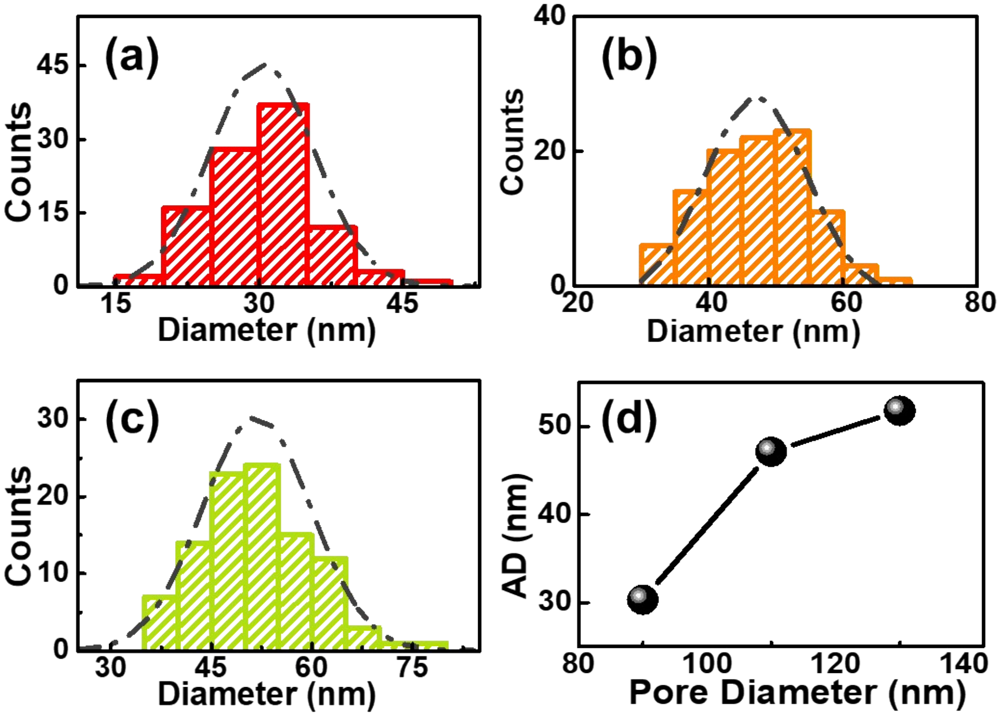

Figure S1 (a) – (c) Statistic particle size distribution diagrams of the self-assembled Au nanostructures (NSs). (d) The average diameter of the Au NSs fabricated on various AAO/Al substrates.

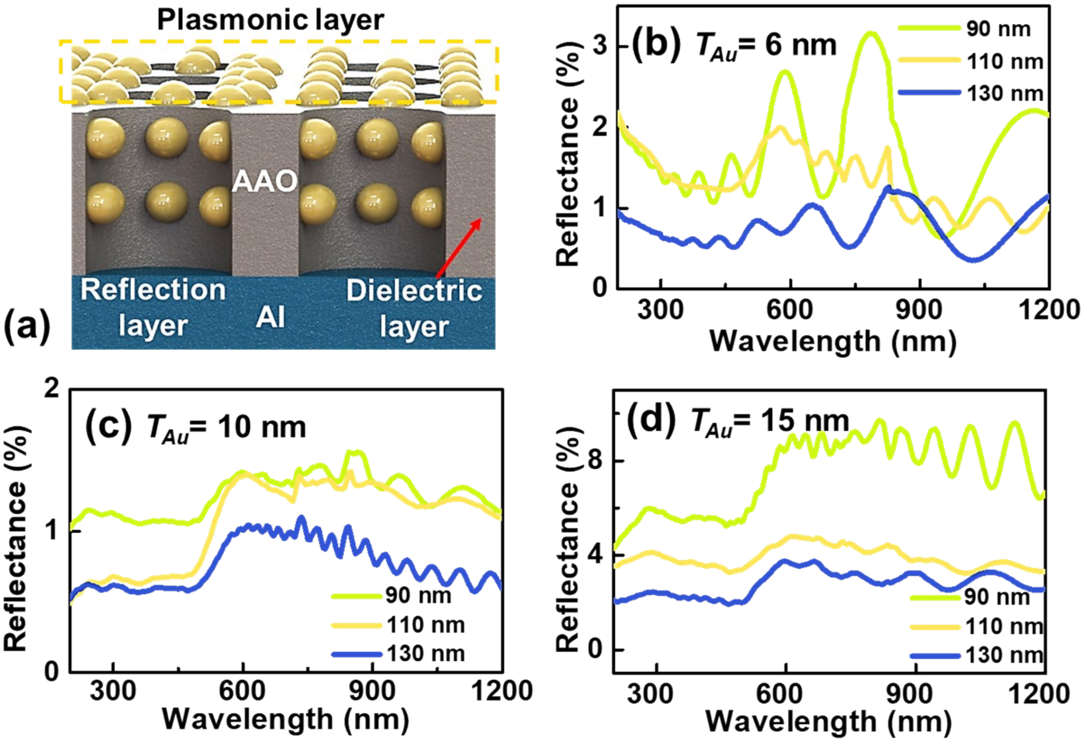

Figure S2 (a) Schematic illustration of Au NPs/AAO/Al 3D plasmonic NSs. Reflection spectra of the 3D plasmonic NSs fabricated with the deposition thicknesses (b) 6, (c) 10, and (d) 15 nm at each D_p.

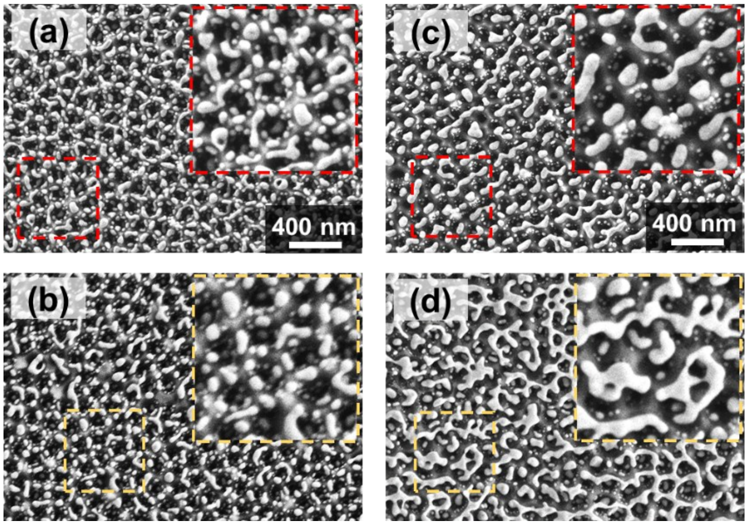

Figure S3 SEM images of the self-assembled Au NSs fabricated with a variation of deposition thicknesses on the AAO/Al substrates with the D_p of 90 (Red color) and 110 (Yellow color). The deposition thicknesses were (a) – (b) 10 nm and (c) – (d) 15 nm.

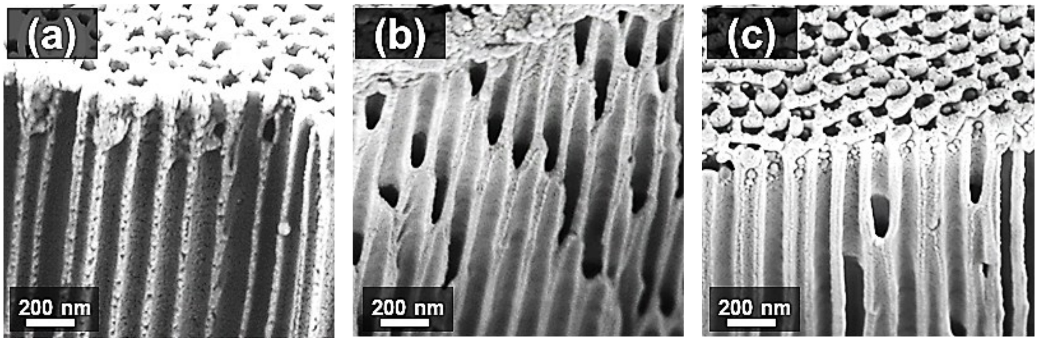

Figure S4 Cross-sectional SEM images of the 3D plasmonc NSs with an identical pore size of 90 nm as a function of Au deposition thicknesses: (a) 6, (b) 10, and (c) 15 nm.

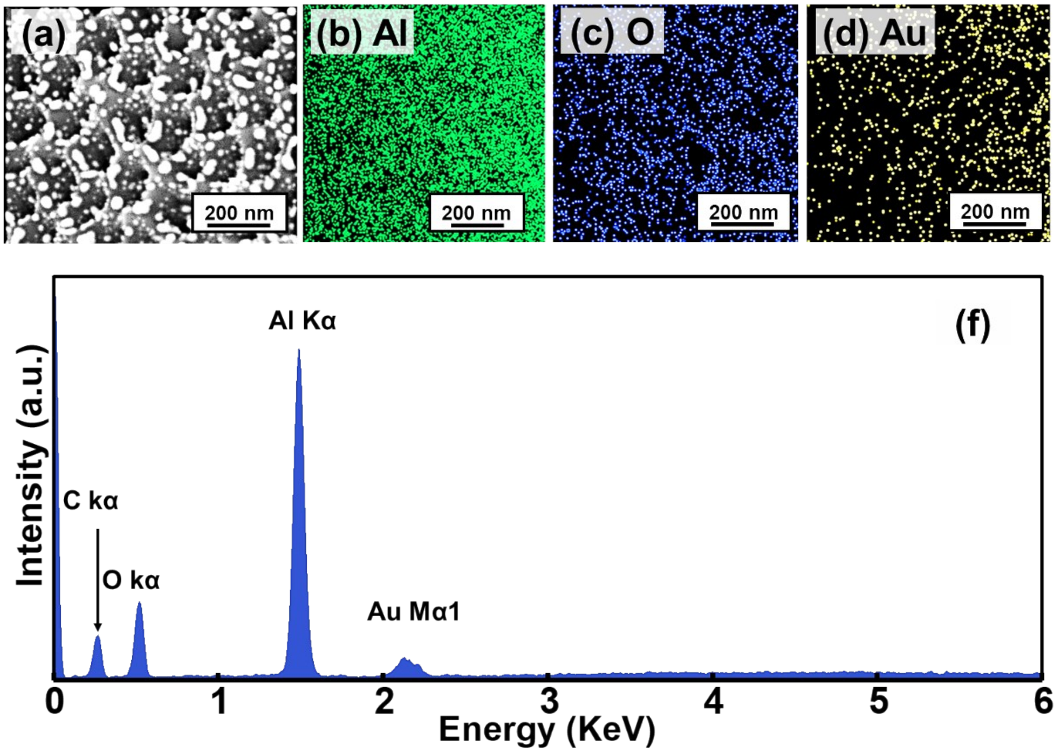

Figure S5 Elemental analysis of the self-assembled Au NPs on AAO/Al substrate by the energy-dispersive X-ray spectroscopy (EDS). (a) SEM image of the sample with 6 nm deposition thicknesses (D_p = 130 nm). (b) – (d) EDS maps of Al, O, and Si. (f) EDS spectra of the sample between 0 and 6 KeV.

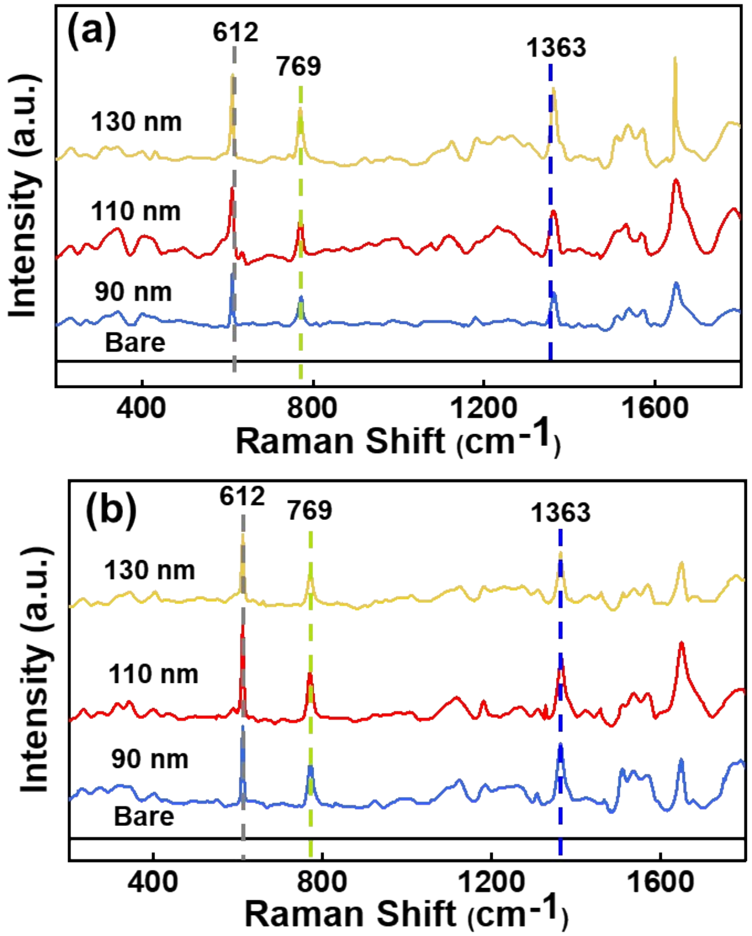

Figure S6 Raman spectra of R6G molecules on the 3D plasmonc NSs with various Au deposition thicknesses: (a) 6 and (b) 15 nm. The D_p varied between 90 and 130 nm.

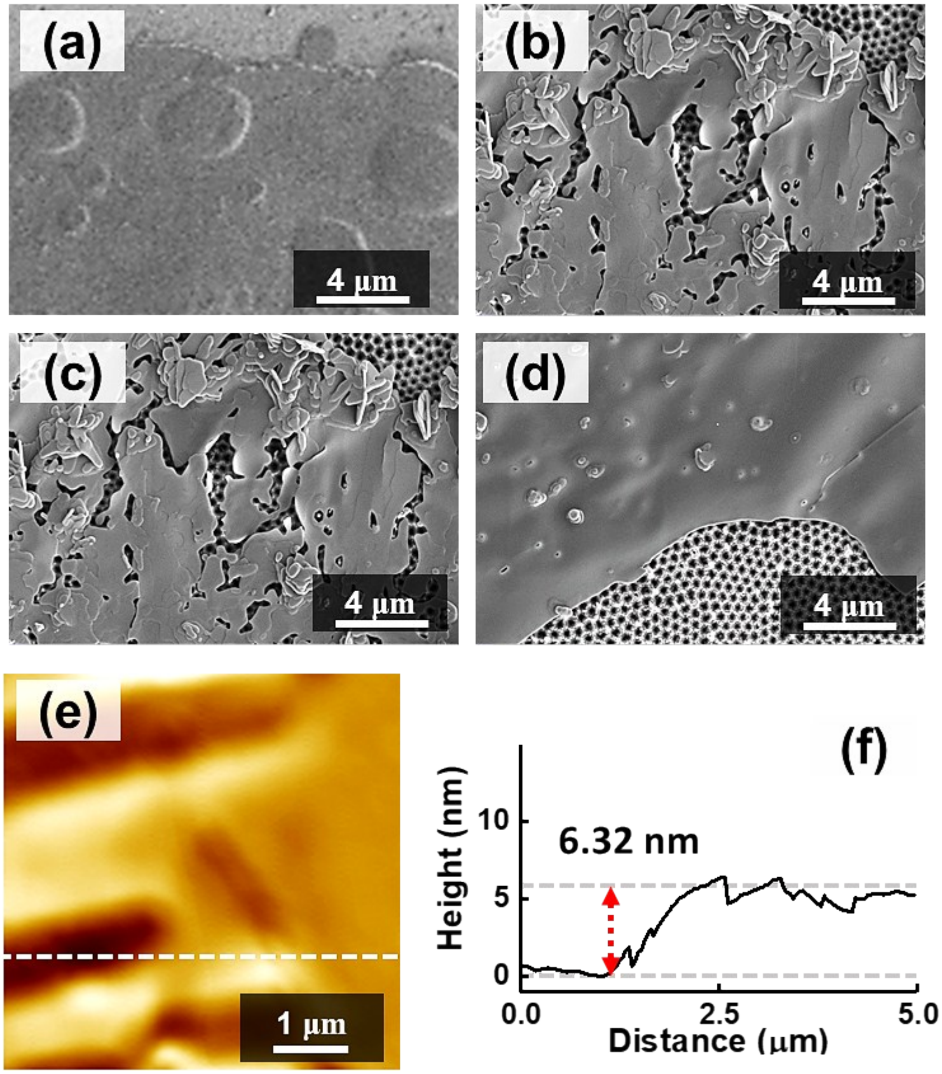

Figure S7 SEM images of p-MSB nanoribbons deposited on (a) glass (Ph1), 3D plasmonc NSs with Au deposition of (b) 6 (Ph2), (c) 10 (Ph3), and (d) 15 nm (Ph4) (D_p = 130 nm). (e) AFM top-views of p-MSB nanoribbons, and (f) cross-sectional line-profile obtained from the area with the white line drawn in the AFM top-view.

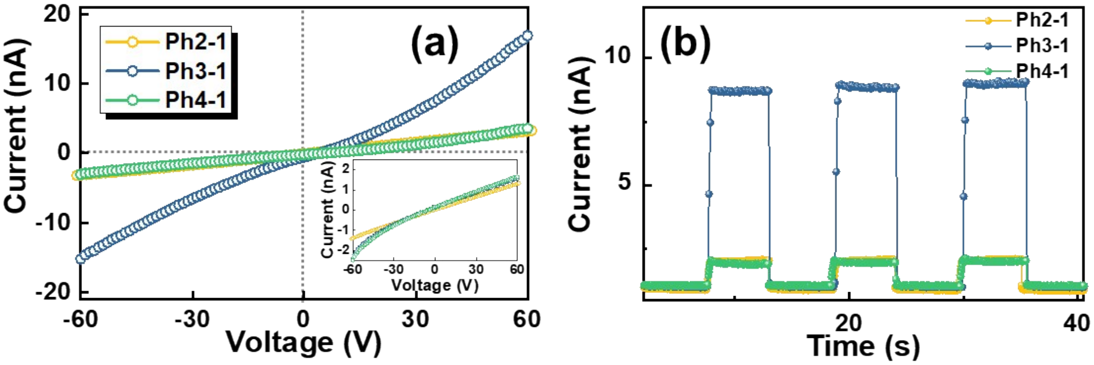

Figure S8 (a) Photocurrent at each bias of the p-MSB ribbon/glass devices under 365 nm UV light illumination (6.9 mW/cm^2). (Inset) Dark current of the devices. (b) Time-resolved photoresponse of the corresponding devices.

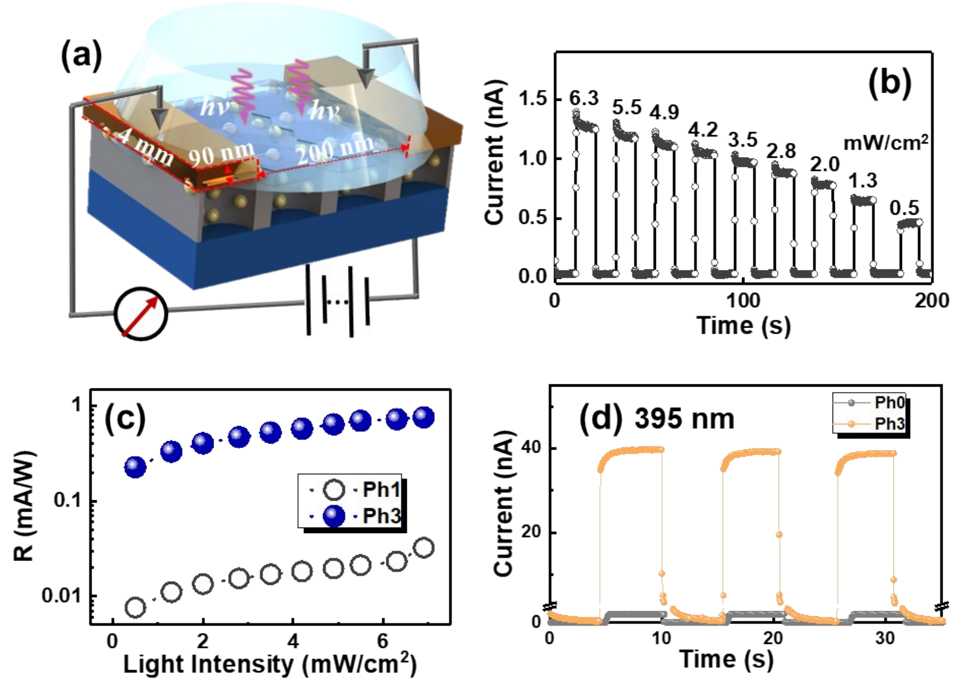

Figure S9 (a) Schematic diagrams of the UV photodetector based on p-MSB ribbon/3D plasmonic NSs. (b) Photoresponse of the Ph1 at various light intensities under 365 nm light illumination. (c) The *R* of the detectors Ph1 and Ph3 at each light intensity. (d) Time-resolved photoresponse of the devices Ph1 and Ph3 under light illumination of 395 nm.

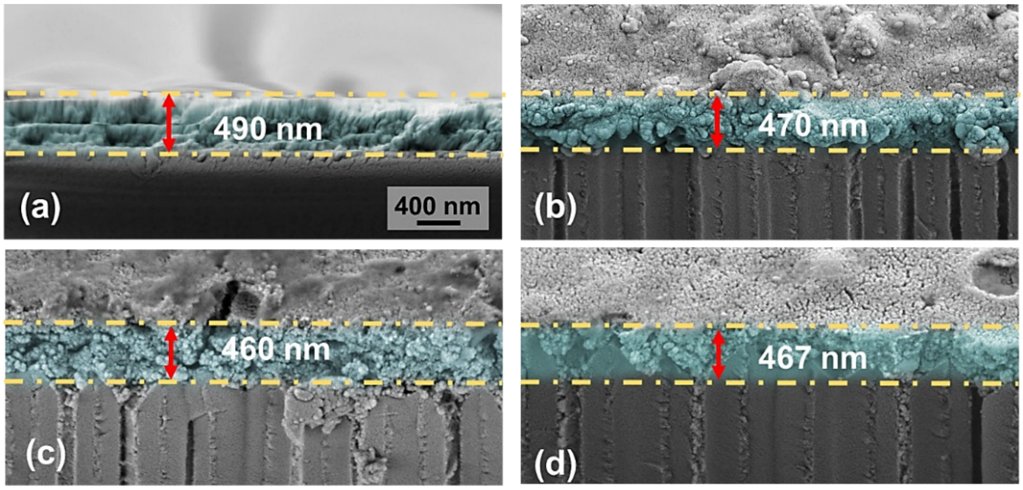

Figure S10 Cross-sectional SEM images of the ZnO CQDs thin films on (a) glass substrate, 3D plasmonic NSs fabricated with (b) 6 nm (c) 10 nm (d) 15 nm Au deposition thicknesses ($D_p = 130$ nm).

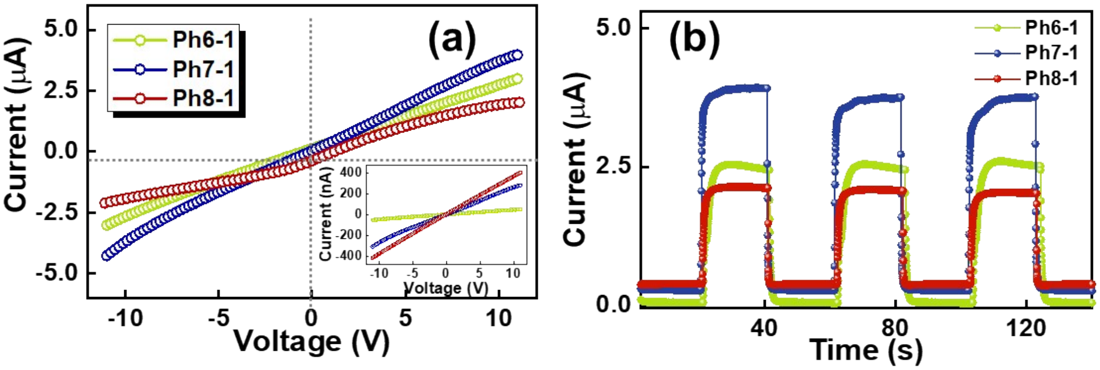

Figure S11 (a) Photocurrent at each bias of the ZnO CQD/glass devices under 365 nm UV light illumination (6.9 mW/cm^2). (Inset) Dark current of the devices. (b) Time-resolved photoresponse.

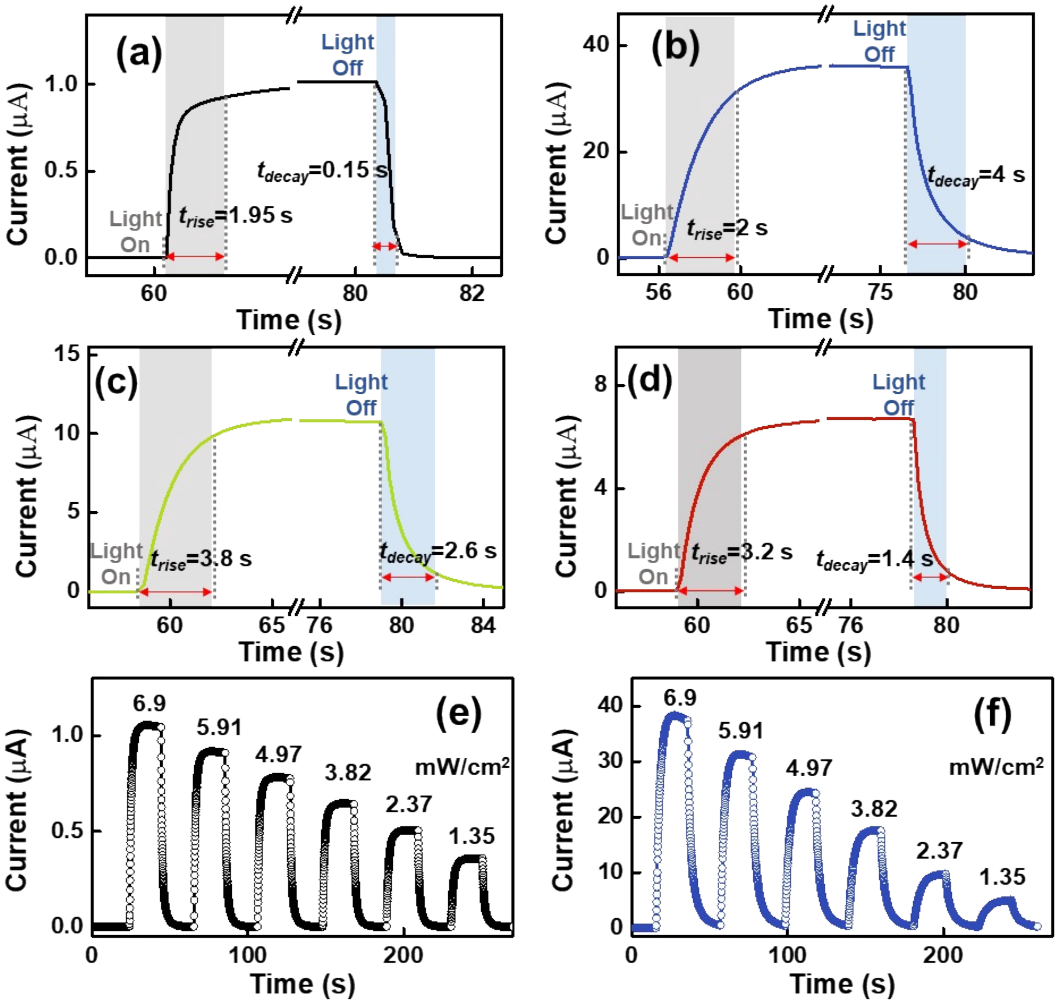

Figure S12 Time-resolved UV photoresponse of the photodetectors (a) Ph5, (b) Ph6, (c) Ph7, (d) Ph8 in a single period. Photoresponse of the (e) Ph5 and (f) Ph7 at various light intensities under 365 nm light illumination.

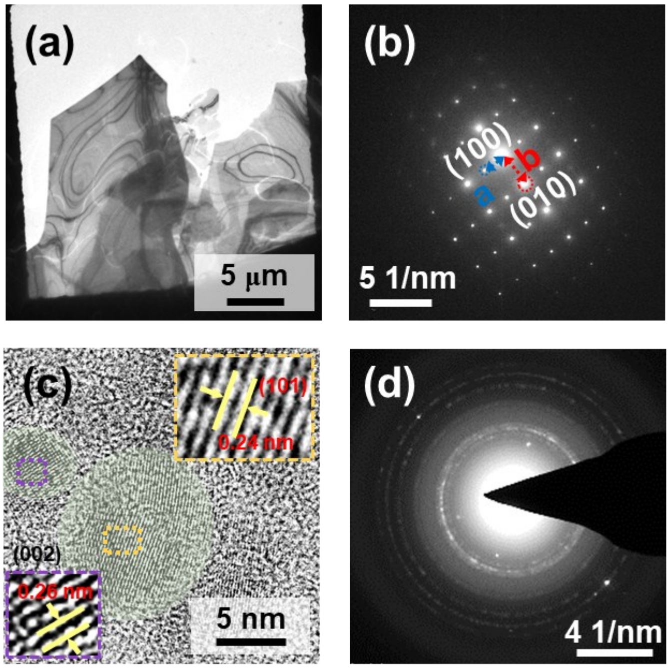

Figure S13 (a) Transmission electron microscope (TEM) images and (b) selected-area electron diffraction (SAED) analysis of p-MSB nanoribbons. (c) High-resolution TEM (HRTEM) images and SADE pattern of the resultant ZnO CQDs.

2. Methods

Preparation of AAO/Al substrate

The high-purity aluminum foils of 1 × 1 cm^2 were initially polished at a constant voltage of 20 V in the mixed solution of perchloric acid and alcohol (V_{Acid}:$V_{Alcohol}$= 1:4), and were anodized at 60 V in 0.3 mol/L oxalic acid at room temperature for 15 min. To subsequent, the irregular-shaped oxidized aluminum films were etched in a mixture of phosphoric and chromic acid at 80 ºC for 0.5 h to define the pores, and then treated with the second anodization under identical condition to form the uniform porous AAO membranes with a pore length of 2 μm. The control over the diameter of the pores was achieved by variation of the reaction duration in 5% H_3PO_4 at room temperature during the following etching process.

Synthesis of p-MSB seeds and ZnO CQDs

The p-MSB oversaturated solution was obtained by disolving 2.0 mg of p-MSB powders (98%, TCI Chemicals) into 10 mL toluene, and was subsequently treated with an ultrasonificantion at 60 °C for 30 min. The p-MSB seeds were obtained during the incubation at room temperature for 30 min, and then heated at 80 °C for 5 min. To maintain the uniformity of the p-MSB seeds, the incubation and heating process was repeated for 3 times. To synthesize ZnO CQDs, 4.46 mmol $Zn(CH_3COO)_2$ (99.99%, aladdin) was dissolved in 42 mL methanol at 60 °C. 7.22 mmol KOH (85%, aladdin) in 23 mL methanol was slowly dripped into the $Zn(CH_3COO)_2$ solution and stirred at 60 °C for 2.25 h. To subsequent, the precipitated product washed by methanol for twice was dispersed into a 6 mL mixture of chloroform and methanol (2:1 by volume) under ultrasonification for 5 min.

Characterization of 3D plasmonic NSs

The morphological characterization of the p-MSB nanoribbons and ZnO CQDs was obtained by high-resolution transmission electron microscope (HRTEM, TF20, FEI Tecnai Corp., America). The scanning electron microscope (GeminiSEM 300, Carl Zeiss Microscopy GmbH, Corp., Germany) was employed for the morphology characterization of the 3D plasmonic NSs and the p-MSB nanoribbons. The optical reflectance spectra were recorded with the UV-VIS-NIR spectrophotometer (UV-3600 PLUS, Japan) within a wavelength range between 200 and 1200 nm. The elements distribution was analyzed with X-ray spectroscopy (EDS) system (GeminiSEM 300, Carl Zeiss Microscopy GmbH, Corp., Germany). Raman spectra were collected by using a 50× objective with a numerical aperture of 0.75 under a laser power of 0.05 mW, which were measured by a Raman spectrometer (LabRAM HR800, Horiba JobinYvon Corp., France) with an excitation of 532 nm laser. To evaluate the SERS, the 10 μL Rhodamine 6G (R6G, SIGMA) aqueous solution of 1×10^{-6} mol/L was directly dropped on the 3D plasmonic NSs following with an incubation of 1 h, and 1×10^{-3} mol/L R6G aqueous solution of 10 μL on glass slide was adapted as a comparison. To verify the reproducibility and homogeneity of the 3D plasmonic NSs, the Raman spectra were average out from the Raman signals randomly acquired from 6 areas for each sample. The performance of the photodetectors was measured by a semiconductor device analyzer (Agilent techhnologies B1500A, America), and illumination was generated through a functional generator (Agilent 33210A) controlled light-emitting diode. Photoluminescence spectra of the devices were acquired by a Raman microscope with an excitation laser of 325 nm (LabRAM HR800, Horiba JobinYvon Corp., France).

Calculation of enhancement factor

Enhancement factor (EF) is considered as the magnitude of increase in Raman scattering cross section when the molecule is adsorbed to a SERS-active substrate. In practical use, EF can be defined by the formula:

$$EF = \frac{I_{SERS}/N_{SERS}}{I_{Raman}/N_{Raman}}$$

where $I_{SERS}$and $I_{Raman}$are the intensities of the SERS and the normal Raman spectra,respectively. Assuming that all the probe molecules within the focused laser spot are excitated and contribute to the SERS spectra and the Raman spectra, N_{SERS} and are N_{Raman} the numbers of molecules adsorbed on SERS-active substrate and glass slide within the focused laser spot, respectively. In the experiments, N_{Raman}/N_{SERS} is estimated from the relation:

$$\frac{N_{Raman}}{N_{SERS}} = \frac{C_{Raman} \times V_{Raman} \times S_{Raman}}{C_{SERS} \times V_{SERS} \times S_{SERS}}$$

where V_{SERS} and C_{SERS} represent a certain volume and concentration of R6G solution dropped on SERS substrates, respectively. Meanwhile, C_{Raman} and V_{Raman} represent the same volume and different concentration of R6G solution dropped on a clean glass slide, respectively. Furthermore, S_{Raman} is the area of focused laser spot on the glass slide and S_{SERS} is the area of focused laser spot on the AAO except the surface area of pore.

Table S1. EF of Raman signals for R6G molecules absorbed on the self-assembled Au nanostructures/AAO/Al substrates with different Au deposition thickness and D_p at 612, 769, 1363 cm^{-1} peaks.

Deposition Thickness (nm)	D_P (nm)	Peak Position (cm^{-1})	Intensity	EF
6	90	612	284	5.3×10^5
	110		394	8.6×10^6
	130		542	1.2×10^7
10	90		1119	2.1×10^7
	110		1449	3.2×10^7
	130		1772	6.1×10^7
15	90		1998	3.7×10^6
	110		2383	5.2×10^7
	130		1690	5.8×10^7
6	90	769	131	3.5×10^5
	110		128	4×10^6
	130		182	9×10^6
10	90		628	1.7×10^6
	110		903	2.8×10^7
	130		1073	5.3×10^7
15	90		1198	3.2×10^6
	110		1238	3.9×10^7
	130		831	4.1×10^7
6	90	1363	196	7.3×10^5
	110		347	1.5×10^7
	130		247	1.7×10^7
10	90		685	1.9×10^7

	110		960	4.2×10^{7}
	130		1476	1×10^{8}
15	90		1531	5.7×10^{6}
	110		1545	6.8×10^{7}
	130		1261	8.7×10^{7}

Table S2. Comparison of the calculated EF between different SERS substrates reported in the literatures.

Substrate	Analyte	EF
Ag-NPs@NiO-NFs@Ni-NR arrays[1]	R6G	2.1×10^6
Nanowire network AAO[2]	Bezene Thiol	5.93×10^6
Hexagonal-Nanopore Array[3]	R6G	8.1×10^6
Au-$CuCl_2$-AAO[4]	R6G	2.3×10^7
MWNTs-AgNPs[5]	4-MBA	4.1×10^7
Hexagonal Au NPs arrays[6]	R6G	4.9× 10^7

Table S3. Characteristic photoresponse parameters of all the p-MSB based photodetectors.

Device	I_{Ph} (nA)	I_{Dark} (nA)	t_{rise} (s)	t_{decay} (s)	R (mA/W)	EQE (%)
Ph1	1.83	0.04	0.22	0.2	0.03	11.04
Ph2	6.16	0.25	0.27	0.1	0.11	36.46
Ph3	42.2	0.26	0.17	0.1	0.76	258.77
Ph4	5.33	0.28	0.27	0.1	0.09	31.16

Table S4. Characteristic photoresponse parameters of all the ZnO based photodetectors.

Device	I_{Ph} (μA)	I_{Dark} (μA)	R (mA/W)	EQE (%)
Ph5	1.02	2.6×10^{-4}	18.47	6.29
Ph6	10.97	6.88×10^{-3}	198.61	67.64
Ph7	36.59	1.02×10^{-1}	661.01	225.13
Ph8	6.73	4.53×10^{-2}	121.1	41.24

References

[1] Q. Zhou, Guo. Meng, Q. Huang, C. Zhu, H. Tang, Y. Qian, B. Chen, B. Chen, Ag-nanoparticles-decorated NiO-nanoflakes grafted Ni-nanorod arrays stuck out of porous AAO as effective SERS substrates. *Phys. Chem Chem. Phys.* **2014**, *16*, 3686.

[2] Q. Jiwei, L. Yudong, Y. Ming, W. Qiang, C. Zongqiang, P. Jingyang, L. Yue, W. Wudeng, Y. Xuanyi, S. Qian, X. Jingjun, Fabrication of nanowire network AAO and its application in SERS. *Nanoscale Res. Lett*. **2013**, *8*, 495.

[3] D. Choi, Y. Choi, S. Hong, T. Kang, L. P. Lee, Self-Organized Hexagonal-Nanopore SERS Array. *Small* **2010**, *6*, 1741.

[4] C. Sui, K. Wang, S. Wang, J. Ren, X. Bai, J. Bai SERS activity with tenfold detection limit optimization on a type of nanoporous AAO-based complex multilayer substrate. *Nanoscale* **2016**, *8*, 5920.

[5] J. Zhang, X. Zhang, S. Chen, T. Gong, Y. Zhu, Surface-enhanced Raman scattering properties of multi-walled carbon nanotubes arrays-Ag nanoparticles. *Carbon* **2016**, *100*, 395.

[6] Z. Yi, X. Ye, J. Luo, X. Kang, Y. Yi, Y. Yi, J. Huang, X. Jiang, Y. Tang, Ordered Hexagonal Nanoplasmonic Au Nanoparticle Arrays: AAO-Assisted Thermal Treatment Synthesis and Application as Surface-Enhanced Raman Scattering Substrates. *Plasmonics* **2017**, *12*, 2013.